Environmental Pollution 281 (2021) 117008

Contents lists available at ScienceDirect

Environmental Pollution

journal homepage: www.elsevier.com/locate/envpol

Contamination levels and habitat use influence Hg accumulation and stable isotope ratios in the European seabass *Dicentrarchus labrax*☆

Marianna Pinzone [a, 1], Alice Cransveld [a, 1], Emmanuel Tessier [b], Sylvain Bérail [b], Joseph Schnitzler [a, c], Krishna Das [a, *], David Amouroux [b]

[a] Freshwater and Oceanic Sciences Unit of Research (FOCUS), Laboratory of Oceanology, University of Liège, B6c Allée du 6 Août, 4000, Liège, Belgium
[b] Universite de Pau et des Pays de l'Adour, E2S UPPA, CNRS, Institut des Sciences Analytiques et de Physico-chimie pour l'Environnement et les Matériaux (IPREM), Technopôle Helioparc, 2 Avenue Pierre Angot, 64053, Pau Cedex 09, France
[c] Institute for Terrestrial and Aquatic Wildlife Research, University of Veterinary Medicine of Hannover, Foundation, Werftstraße 6, 25761, Büsum, Schleswig-Holstein, Germany

ARTICLE INFO

Article history:
Received 21 December 2020
Received in revised form
15 March 2021
Accepted 20 March 2021
Available online 24 March 2021

Keywords:
Multi-tissue
Stable isotopes
Seabass
Demethylation
Contamination level

ABSTRACT

Hg accumulation in marine organisms depends strongly on *in situ* water or sediment biogeochemistry and levels of Hg pollution. To predict the rates of Hg exposure in human communities, it is important to understand Hg assimilation and processing within commercially harvested marine fish, like the European seabass *Dicentrarchus labrax*. Previously, values of Δ^{199}Hg and δ^{202}Hg in muscle tissue successfully discriminated between seven populations of European seabass. In the present study, a multi-tissue approach was developed to assess the underlying processes behind such discrimination.

We determined total Hg content (THg), the proportion of monomethyl-Hg (%MeHg), and Hg isotopic composition (e.g. Δ^{199}Hg and δ^{202}Hg) in seabass liver. We compared this to the previously published data on muscle tissue and local anthropogenic Hg inputs.

The first important finding of this study showed an increase of both %MeHg and δ^{202}Hg values in muscle compared to liver in all populations, suggesting the occurrence of internal MeHg demethylation in seabass. This is the first evidence of such a process occurring in this species. Values for mass-dependent (MDF, δ^{202}Hg) and mass-independent (MIF, Δ^{199}Hg) isotopic fractionation in liver and muscle accorded with data observed in estuarine fish (MDF, 0–1‰ and MIF, 0–0.7‰). Black Sea seabass stood out from other regions, presenting higher MIF values ($\approx$1.5‰) in muscle and very low MDF ($\approx$-1‰) in liver. This second finding suggests that under low Hg bioaccumulation, Hg isotopic composition may allow the detection of a shift in the habitat use of juvenile fish, such as for first-year Black Sea seabass.

Our study supports the multi-tissue approach as a valid tool for refining the analysis of Hg sourcing and metabolism in a marine fish. The study's major outcome indicates that Hg levels of pollution and fish foraging location are the main factors influencing Hg species accumulation and isotopic fractionation in the organisms.

1. Introduction

Monomethyl-Hg (MeHg), the most toxic form of Hg, is readily bioavailable in the marine environment and bioaccumulates in the food web (Hong et al., 2012; Lang et al., 2017; Mozaffarian and Rimm, 2008; Renzoni et al., 1998; UNEP, 2018, 2013). Several processes modulate MeHg bioavailability (Du et al., 2019). In surface waters, sunlight radiation can control the degradation of methylated Hg species. Several mechanisms are proposed to cause MeHg photodegradation (Luo et al., 2020). It is generally recognized that this process is induced by ultraviolet light (UV-A and UV-B, 280–400 nm) (Lehnherr and Louis, 2009) and controlled by the type and abundance of MeHg-binding ligands (e.g. OH^-, $^1O_2$, DOM, organic thiols or chloride complexes) in the water column (Luo et al., 2020; Zhang and Hsu-kim, 2010). In deeper layers, MeHg is mostly processed by microbial activity, either in the aphotic water column during microbial remineralization of settling organic

☆ This paper has been recommended for acceptance by Wen-Xiong Wang.
* Corresponding author.
E-mail address: Krishna.das@uliege.be (K. Das).
[1] Both authors contributed equally to the work.

https://doi.org/10.1016/j.envpol.2021.117008
0269-7491/

matter, or in anoxic conditions at the sea bottom (Gworek et al., 2016; Li et al., 2016; Mason et al., 2001; Sunderland et al., 2010). Iron- and sulfur-reducing bacteria (IRB and SRB, respectively) as well as methanogens are the main groups of prokaryotes responsible for Hg processing in anoxic conditions (Bystrom, 2008; Lu et al., 2016; Regnell and Watras, 2019).

Consequently, local climatic and oceanographic features, combined with growing anthropogenic activities, might alter the complex Hg cycle, with unknown consequences for its marine life. Apex predators such as marine mammals, seabirds or carnivorous fish can accumulate extremely high levels of Hg, being at the top of marine food webs (Sonke et al., 2013). For this reason, understanding Hg uptake and accumulation in these animals is a priority. Such urgency is also related to the fact that most species of edible carnivorous fish (tuna, cod, seabass etc.) are commonly consumed by humans (Serrell et al., 2012).

Recently, the use of stable isotopes of Hg was proven useful for discriminating between potential Hg sources and accumulation in aquatic habitats (Bergquist and Blum, 2009; Cransveld et al., 2017; Gantner et al., 2009; Gehrke et al., 2011; Kwon et al., 2014a; Perrot et al., 2010; Point et al., 2011; Senn et al., 2010; Sherman and Blum, 2013; Yin et al., 2016). The seven stable isotopes of Hg (Z = 196, 198, 199, 200, 201, 202 and 204) can undergo mass-dependent fractionation (MDF) and mass-independent fractionation (MIF) (Bergquist and Blum, 2009). MDF (mostly represented by δ^{202}Hg) occurs during a variety of chemical, physical and biological reactions, and has been used to detail the processes controlling Hg transport, transformation and bioaccumulation (Bergquist and Blum, 2009). More specifically, MDF can be used to trace Hg transfer from the environment throughout the food web (Tsui et al., 2019). The latest constraints to the interpretation of MDF data include its quantification at higher trophic levels, where fractionation rates are complicated by biotransformation processes occurring within the organisms (e.g. demethylation) (Tsui et al., 2019). MIF is not modified throughout the food web and thus provides a unique fingerprint of primary Hg sources in the marine environment (Obrist et al., 2018). The occurrence of MIF (represented mostly by Δ^{199}Hg and Δ^{201}Hg values) has been attributed to all photochemical reactions, such as photochemical reduction of Hg^{2+} (Bergquist and Blum, 2007), and photodemethylation of DOM-associated MeHg in both the water column (Chandan et al., 2015) and marine phytoplankton cells (Kritee et al., 2018). Finally, even-mass isotopes (Δ^{200}Hg, Δ^{204}Hg) are dependent on the atmospheric cycle of Hg, discriminating for example between precipitation sources (e.g. snow *vs.* rain) (Gratz et al., 2010; Sherman et al., 2010).

We recently measured MDF and MIF values in seabass muscle (*Dicentrachus labrax*) to discriminate between different sub-populations in Europe and in the Black Sea (Cransveld et al., 2017). We highlighted a large heterogeneity in Hg MDF and MIF between the seven sampling regions, and suggested hepatic MeHg demethylation or different Hg sourcing as potential causes (Cransveld et al., 2017). However, the exclusive use of muscle as the monitoring tissue did not allow more extensive interpretation.

Indeed, while Hg monitoring studies often focus on muscle, the analysis of Hg isotopes and speciation in liver can bring additional perspectives (Tsui et al., 2019). Each tissue indeed exhibits specific concentrations and proportions of Hg species (Mieiro et al., 2011; Pentreath, 1976), depending on several factors: tissue composition (proteins, lipids, carbohydrates), turnover rate, and the food regime of fish (Jardine et al., 2006; Maury-Brachet et al., 2006; Perga and Gerdeaux, 2005; Wang and Wong, 2003). For this reason, the inclusion of more tissues in the assessment of Hg stable isotopes in a single organism was proposed as a valid and necessary approach that may offer a more comprehensive picture of the dynamics of contaminant uptake (Jardine et al., 2006; Tsui et al., 2019) and internal processing by marine organisms (Kwon et al., 2012, 2016). In this regard, liver is the key tissue. In marine mammals, aquatic birds and some fish species, the liver is demonstrated to act as detoxifying organ (Booth and Zeller, 2005; Eagles-Smith et al., 2009; Feng et al., 2015; Gonzalez et al., 2005; Wagemann et al., 1998). Thus, the combination of stable isotope analysis in both muscle and liver of marine predators could allow a complete understanding of MeHg sources and processing in both wildlife and the wider environment.

Therefore, to understand Hg sources and organotropism of this species around Europe, in this study we compared THg, %MeHg and Hg isotope composition (MIF and MDF) in the liver of wild seabass *Dicentrarchus labrax* with previously published muscle data (Cransveld et al., 2017). Specifically, we wanted to test three distinct hypotheses: (1) The use of a multi-tissue approach improves isotopic tracing of Hg biogeochemical processes and sources between natural ecosystems, in comparison with the singular analysis of muscle; (2) MeHg demethylation may occur in seabass liver and its rates can be dependent on the extent of local mercury pollution; (3) the peculiar biogeochemical settings of each sampling site may determine the particular sourcing of MeHg in local seabass.

2. Materials and method

2.1. Sample collection

Sampling of the seabass *Dicentrachus labrax* used in the present study has been described previously (Cransveld et al., 2017). All the biometric information available for the sampled fish is summarized in Table 1. All fish were juveniles, sampled at their nursery sites. Fish were collected between 2012 and 2014 from seven coastal sites throughout Europe: the North Sea (NS), the Northern Aegean Sea (AES), the Seine Estuary (SE), the Northern Adriatic Sea (NAS), the Turkish coast of the Black Sea (BS), and two different sites at the Ria de Aveiro in Portugal (a "reference" site and a "contaminated" site – RAR and RAC respectively). These sites are subjected to different levels of Hg pollution because of their specific industrial origin. Details about each site are given in Table 1 and in the Supporting Information of Cransveld et al. (2017). Sites were separated into "low", "moderate" and "highly" polluted categories, based on the statistical differences published on muscle concentrations (Cransveld et al., 2017). Figure S1 shows these three groups as *a*, *b* and *c*. After sampling, fish were kept in freezers at −20 °C. Prior to dissection, fish were measured and weighed. Liver was sampled, freeze-dried and ground into powder.

2.2. Analyses

THg concentrations were determined in the liver of fish through the use of a Milestone Direct Mercury Analyzer 80 (Habran et al., 2012), using the US EPA Method 7473, validated for solid samples. THg concentrations are expressed as ng g^{-1} dry weight (DW). Quality assurance methods included measuring blanks (HCl 1%), standard solutions (100 ng $Hg.ml^{-1}$), triplicates of samples, and certified reference material NRC-DORM-2 (certified T-Hg value = 4640 ± 260 ng g^{-1} dw). CRM recovery percentages ranged from 89% to 110% (Table S1).

MeHg concentrations were determined by isotope dilution-gas chromatography, inductively-coupled-plasma mass spectrometer (ID-GC-ICP-MS), following microwave-assisted extraction and aqueous phase derivatization, as detailed elsewhere (Cransveld et al., 2017; Rodríguez Martín-Doimeadios et al., 2002). For the extraction, between 50 and 100 mg of the liver sample was weighed. BCR CRM-464 (tuna fish muscle certified for MeHg and THg concentration) and DOLT-4 (dogfish liver) were used as

Table 1
Summary of fish biometric information per sampling area. Information about local Hg sources at the sampling sites are extrapolated from literature and supporting information in Cransveld et al. (2017). Old pollution sources which are not active anymore are shown in italics.

Sampling Site	Standard length (cm)	Body mass (g)	Estimated age range (years)	Pollution sources	Definition[a]
AGEAN SEA **AES**	28 ± 1 (25–30) n = 10	272 ± 48 (205–380) n = 10	2	Protected by the Ramsar convention	Low Pollution
NORTH SEA **NS**	26 ± 6 (16–30) n = 10	192 ± 90 (43–278) n = 10	1–3	Interland industry Coastal urbanism	Moderate Pollution
SEINE ESTUARY **SE**	33 ± 2 (30–35) n = 10	487 ± 66 (350–563) n = 10	3–4	Interland industry Coastal urbanism	Moderate Pollution
BLACK SEA **BS**	21 ± 2 (18–24) n = 10	140 ± 24 (110–170) n = 10	1–2	Interland industry and agriculture	Low Pollution
NORTHERN ADRIATIC SEA **NAS**	22 ± 1 (20–23) n = 9	123 ± 20 (89–149) n = 9	1	*Idrija mercury mine* *Chlor-alkali plant* Coastal industry	High Pollution
RIA DE AVEIRO REFERENCE **RAR**	21 ± 4 (17–26) n = 10	106 ± 60 (55–217) n = 10	1–2	(Lagoon outlet) Coastal industry and urban development	Moderate Pollution
RIA DE AVEIRO CONTAMINATED **RAC**	17 ± 1 (16–18) n = 12	59 ± 10 (45–77) n = 12	1	(Laranjio Basin) *Chlor-alkali plant* Coastal industry and urban development	High Pollution

[a] We separated the sampling sites into three categories: "Low Pollution" for all the sites presenting THg = <200 ng.g^{-1} dw, "Moderate Pollution" when THg ranged between 500 and 1500 ng.g^{-1} dw, and "High Pollution" when THg = >1500 ng.g^{-1} dw, based on the statistical difference reported for muscle concentrations (*a*, *b* and *c* in Figure S1).

reference materials. Certified and obtained THg and MeHg values are shown in Table S2. All solutions were prepared using ultrapure water (18 MΩ cm, Millipore). Trace Metal Grade acids HNO_3 and HCl from Fisher Scientific (Illkirch, France) and ultrapure H_2O_2 (67–70%, ULTREX® II, J.T.Baker) were used for the preparation of all the samples, standards and blanks. Between 20 and 570 mg of liver samples were mineralized in quartz vials with trace metal grade nitric acid (HNO_3), using a HPA High Pressure Asher (Anton Paar, Austria). Then, ultrapure hydrogen peroxide (H_2O_2) was added, and samples went through a digestion process for three more hours on a hot block (80 °C) to ensure full mineralization of organic matter. The samples were then diluted to obtain a final Hg concentration of 1 ng g^{-1} in an acid solution, which was adjusted to contain 10% HNO_3 and 2% HCl. Blanks were prepared by pouring nitric acid in vials, without samples. CRM recovery percentages ranged from 74% to 94% (Table S2).

Mercury isotopic composition analysis was performed using cold vapor generation (CVG) with multi-collector-inductively coupled plasma-mass spectrometer (MC-ICP-MS, Nu Instruments) (Cransveld et al., 2017). A desolvation/nebulization system from Nu Instrument was used to introduce NIST-SRM-997 thallium for instrumental mass-bias correction using the exponential fractionation law. Reference material NIST RM 8610 (former UM-Almaden), ERM-CE-464 and DOLT-4 were used as secondary standards. The resulting Hg isotopic composition is presented in Table S3.

We used a standard-sample bracketing system to calculate δ values (in ‰) relative to the reference standard NIST SRM 3133 mercury spectrometric solution. Isotope ^{198}Hg was used as the reference for ratio determination of all other Hg isotopes, using the following equations:

$$\delta^{xxx}Hg = \left[\frac{\left(^{xxx}Hg/^{198}Hg\right)_{sample}}{\left(^{xxx}Hg/^{198}Hg\right)_{NIST\ 3133}} - 1\right] \times 1000$$

MDF processes will be represented by δ^{202}Hg values. MIF processes will be calculated and represented as follows for odd (1 & 2) and even (3 & 4) isotopes:

$$\Delta^{199}Hg = \delta^{199}Hg_{observed} - \delta^{199}Hg_{predicted} = \delta^{199}Hg_{observed} - \left(\delta^{202}Hg \times 0.252\right) \quad (1)$$

$$\Delta^{201}Hg = \delta^{201}Hg_{observed} - \delta^{201}Hg_{predicted} = \delta^{201}Hg_{observed} - \left(\delta^{202}Hg \times 0.752\right) \quad (2)$$

$$\Delta^{200}Hg = \delta^{200}Hg_{observed} - \delta^{200}Hg_{predicted} = \delta^{200}Hg_{observed} - \left(\delta^{202}Hg \times 0.502\right) \quad (3)$$

$$\Delta^{204}Hg = \delta^{204}Hg_{observed} - \delta^{204}Hg_{predicted} = \delta^{204}Hg_{observed} - \left(\delta^{202}Hg \times 1.493\right) \quad (4)$$

A more detailed description of Hg speciation and isotope analysis, including quality assurance and method validation, can be found in the Supporting Information of this work and in previous literature (Cransveld et al., 2017; Renedo et al., 2018).

2.3. Statistics

Since the sampling size was small (n ≤ 12) for each sampling location, we used non-parametric tests for statistical analyses. Statistical significance was set at α = 0.01 (instead of 0.05). Differences between groups with *p*-values between 0.05 and 0.01 were reported in the results but not interpreted as effective. To test variance amongst sampling sites, we used the non-parametric Kruskal-Wallis (K–W) for each parameter separately. We used the Spearman's ρ to correlate concentrations and isotopic values. Finally, to test the difference between variables measured in muscle and in liver, we used the paired samples Wilcoxon test.

3. Results

3.1. THg and MeHg concentrations

Concentrations of THg in muscle and liver differed significantly between sampling sites (K–W; H = 50.81; $p < 0.0001$ and H = 46.60; $p < 0.0001$) (Table 2). These were separated into three groups: the most contaminated NAS and RAC, the intermediate RAR, NS and SE, and the least contaminated AES and BS (Figure S1). In liver, such differences were less important, but THg and MeHg concentrations followed the same profile (Figure S1-Right and Table 2).

Liver %MeHg differed significantly between sampling sites (K–W; H = 41.00; $p < 0.0001$), ranging from 7% in BS to 82% in NAS (Figure S2b). For the whole dataset (n = 62), THg was moderately correlated to %MeHg (r = 0.51; $p = 0.0001$). In muscle, %MeHg varied less, with a significant difference observed only between SE and NAS and AES (K–W; H = 36.91; $p < 0.0001$). Percentage values ranged between 71% in NAS and 93% in SE (Figure S2a). No correlation was found between the %MeHg in muscle and THg levels among regions (Spearman; r = 0.13; $p = 0.324$).

3.2. Hg stable isotope composition

Hepatic δ^{202}Hg and Δ^{199}Hg values varied significantly between sampling locations (K–W; H = 50.69; $p < 0.0001$ and H = 38.55; $p < 0.0001$, respectively) (Table 2). There was strong correlation between Δ^{199}Hg and Δ^{201}Hg (Spearman; r = 0.95; $p < 0.0001$) for all sites, and the value of the slope of the regression line was 1.30 ± 0.02 (Fig. 1a). A positive correlation between Δ^{199}Hg and δ^{202}Hg values was found only for SE (p = 0.001, ρ = 0.661), BS (p = 0.005, ρ = 0.628) and RAC (p = 0.016, ρ = 0.530) (Fig. 1b). Only BS fish showed a positive correlation between Δ^{199}Hg and δ^{202}Hg values and %MeHg in both tissues (respectively: p < 0.0001, ρ = 0.767 and p = 0.0013, ρ = 0.698).

Only a weak difference was observed in hepatic Δ^{200}Hg values (Figure S3a; K–W, H = 14.33 and $p = 0.023$), with AES presenting higher even-MIF than RAC and SE. Δ^{204}Hg values differed slightly more (Figure S3b; K–W, H = 19.83 and $p = 0.003$) with RAC presenting significantly smaller MIF than RAR and SE. The great variation found in even-MIF values did not allow us to discriminate between specific atmospheric sources in seabass populations and will not be discussed further. Raw data and a short discussion are given in the Supporting Information (Section S2.a, Table S4; Figure S3a and b).

When compared with muscle results published in Cransveld et al. (2017), the difference between δ^{202}Hg $_{muscle}$ and δ^{202}Hg $_{liver}$ ranged from 0.04‰ in NAS to 1.08‰ in BS. δ^{202}Hg values differed significantly between the two tissues only in BS seabass (K–W, H = 84.9, p = 0.003). The difference between Δ^{199}Hg $_{muscle}$ and Δ^{199}Hg $_{liver}$ went from −0.02‰ in NAS to 1.13‰ in BS. As before, Δ^{199}Hg values differed only in BS seabass (K–W, H = 95.5, p < 0.0001). δ^{15}N, δ^{13}C values and trophic position (TL) in the different seabass populations were presented elsewhere (Cransveld et al., 2017). No correlation was found between carbon and nitrogen isotope ratios in seabass muscle and %MeHg in liver. For this reason, we do not discuss these results further. More details can be found in paragraph S2.b.

4. Discussion

4.1. Evidence of Hg demethylation in seabass across Europe

The lowest THg muscle and liver concentrations were observed in Greece and the Black Sea (AES and BS sites), while the highest

Table 2
THg and MeHg concentrations (ng.g^{-1}, dw), %MeHg and Hg isotopic ratios (as δ and Δ values, ‰) in liver of *Dicentrarchus labrax* from seven sampling sites across Europe. All values are expressed as mean ± standard deviation (SD), median (minimum–maximum) and n = number of analyzed samples.

SAMPLING SITE	[THg]	[MeHg]	%MeHg	δ^{202}Hg	Δ^{199}Hg	Δ^{200}Hg	Δ^{201}Hg	Δ^{204}Hg
AGEAN SEA	166 ± 37	89 ± 34	52 ± 15	−0.57 ± 0.10	0.67 ± 0.17	0.05 ± 0.03	0.39 ± 0.06	−0.12 ± 0.08
AES	182 (101–203)	86 (46–154)	52 (31–83)	−0.56 (−0.75–−0.42)	0.62 (0.49–1.03)	0.05 (0.00–0.09)	0.40 (0.29–0.49)	−0.09 (−0.24–−0.01)
	n = 10	n = 9	n = 9	n = 10	n = 10	n = 10	n = 10	n = 10
NORTH SEA	840 ± 575	326 ± 179	42 ± 10	−0.53 ± 0.18	0.32 ± 0.16	0.02 ± 0.03	0.12 ± 0.07	−0.03 ± 0.04
NS	827 (208–1498)	375 (86 –457)	42 (30–54)	−0.51 (−0.76–−0.32)	0.31 (0.15–0.52)	0.02 (−0.01–0.06)	0.15 (0.03–0.17)	−0.02 (−0.08–0.02)
	n = 4	n = 4	n = 4	n = 4	n = 4	n = 4	n = 4	n = 4
SEINE ESTUARY	1031 ± 153	512 ± 111	50 ± 10	−0.25 ± 0.08	0.21 ± 0.08	0.001 ± 0.03	0.19 ± 0.07	0.01 ± 0.06
SE	1016 (769–1228)	536 (277–646)	49 (36–70)	−0.26 (−0.37–−0.13)	0.20 (0.08–0.38)	0.00 (−0.05–0.05)	0.17 (0.12–0.36)	−0.01 (−0.07–0.09)
	n=10	n = 10	n = 10	n = 10	n = 10	n = 10	n = 10	n = 10
BLACK SEA	180 ± 47	13 ± 3	7.5 ± 2.3	−0.98 ± 0.17	0.17 ± 0.05	0.02 ± 0.03	0.09 ± 0.04	−0.04 ± 0.08
BS	177 (99–268)	12 (10–20)	7.3 (4.8–11)	−0.94 (−1.41–−0.85)	0.18 (0.10–0.24)	0.03 (−0.05–0.04)	0.08 (0.05–0.17)	−0.04 (−0.12–0.07)
	n=9	n = 9	n=9	n = 9	n = 9	n = 9	n = 9	n = 9
NORTHERN	1714 ± 1255	1160 ± 883	67 ± 8.1	−0.01 ± 0.14	0.54 ± 0.13	0.01 ± 0.04	0.40 ± 0.09	0.01 ± 0.21
ADRIATIC SEA	1174 (884–4432)	877 (506–3115)	66 (54–8)	−0.05 (−0.17–0.27)	0.59 (0.37–0.69)	0.02 (−0.07–0.07)	0.42 (0.29–0.50)	0.07 (−0.41–0.26)
NAS	n = 8	n= 8	n = 8	n = 8	n = 8	n = 8	n = 8	n = 8
RIA DE AVEIRO	1368 ± 804	737 ± 431	27 ± 21	−0.09 ± 0.14	0.42 ± 0.10	0.01 ± 0.03	0.33 ± 0.10	0.13 ± 0.21
REFERENCE	1274 (333–2243)	887 (227–1122)	20 (10–50)	−0.13 (−0.23–0.11)	0.41 (0.29–0.55)	0.00 (−0.03–0.06)	0.31 (0.19–0.46)	0.20 (−0.17–0.34)
RAR	n = 6	n = 5	n=3	n = 6	n = 6	n = 6	n = 6	n = 6
RIA DE AVEIRO	2888 ± 468	1088 ± 680	69 ± 7	0.11 ± 0.10	0.20 ± 0.07	0.002 ± 0.02	0.14 ± 0.05	−0.17 ± 0.15
CONTAMINATED	2785 (2309–3515)	1220 (119–1903)	67 (57–80)	0.12 (−0.13–0.22)	0.19 (0.03–0.30)	0.01 (−0.03–0.03)	0.14 (0.05–0.21)	−0.18 (−0.33–0.20)
RAC	n = 10	n= 10	n = 9	n = 10	n = 10	n = 10	n = 10	n = 10

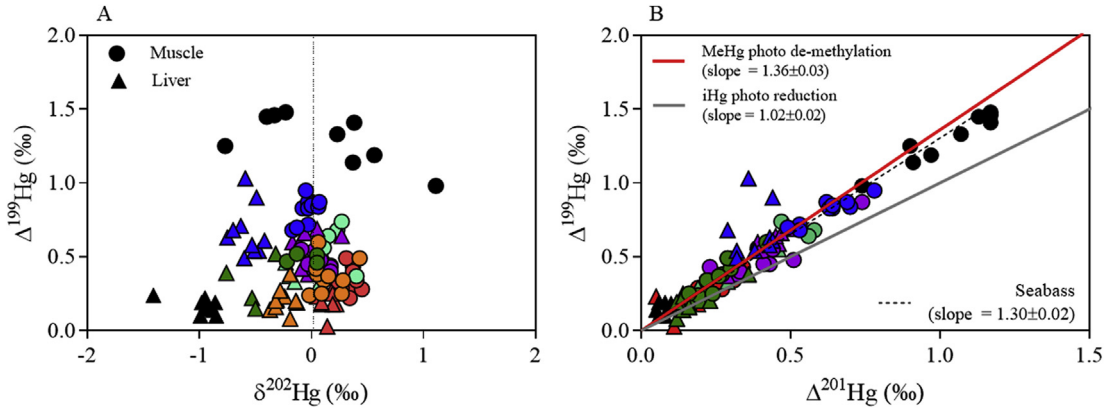

Fig. 1. MIF *vs.* MDF plot (**A**) and MIF *vs.* MIF plot (**B**) of muscle (circle) and liver (triangle) of European seabass (*D. labrax*) from AES (blue), NS (green), SE (orange), NAS (violet), BS (black), RAR (light green) and RAC (red). Significant correlation is shown by discontinuous regression lines. (For interpretation of the references to colour in this figure legend, the reader is referred to the Web version of this article.)

concentrations were measured in the North Adriatic Sea and Ria d'Aveiro (NAS and RAC sites; Table 2). Liver %MeHg ranged from 7 to 10% in BS, 30–40% in the contaminated area of RAC, and up to 70% in NS, SE and AES. On the other hand, muscle %MeHg was constant around 80–90% across all sites (Cransveld et al., 2017). The different MeHg profile between muscle and liver is in accordance with previous literature and the role that these two tissues have in the fish body (Mieiro et al., 2009). Muscle is often described as the final Hg storage tissue in marine vertebrates, where dietary MeHg is accumulated at a high rate and not metabolized further (Oliveira Ribeiro et al., 1999). This is why %MeHg remains constant. Instead, the extremely variable proportions of MeHg displayed by liver are thought to be an expression of the protective role of this organ (Mieiro et al., 2011; Oliveira Ribeiro et al., 1999). Indeed, in this organ, dietary MeHg binds with Selenium (Se) and is transformed into an inert tiemannite complex (HgSe) (Sonne et al., 2009). In this way, Hg is locally accumulated in a less toxic and non-available inorganic form. Through the application of Hg stable isotope ratios, there is increasing evidence that the liver acts as a Hg detoxification center in fish, as it does in marine mammals or seabirds (Renedo et al., 2021; Wang et al., 2013, 2017).

Hg stable isotopes can undergo MDF during uptake and metabolism of Hg within the organisms (transfer, transformation and excretion) (Li et al., 2020). Important Hg MDF related to MeHg demethylation is now also broadly accepted to occur in fish (Man et al., 2019; Wang and Tan, 2019). MeHg demethylation causing MDF preferentially involves lighter Hg isotopes and generates newly formed iHg, having a lower δ^{202}Hg (Perrot et al., 2015). The remaining non de-methylated MeHg will then have a higher δ^{202}Hg compared to the initially bioaccumulated MeHg (Perrot et al., 2015). Because most iHg is excreted, the fractionation (MDF) caused by demethylation is probably more observable in MeHg-rich tissues like muscle (Gehrke et al., 2011; Kwon et al., 2014a; Sherman and Blum, 2013). Since liver is the center of *in vivo* demethylation and therefore contains a lower proportion of MeHg, it will display lower δ^{202}Hg values than muscle. Consequently, a large shift in δ^{202}Hg values and %MeHg between muscle and liver tissues of seabass could infer the occurrence of MeHg demethylation in the liver of the fish (Wang et al., 2013). All our sampling areas showed a significant difference in %MeHg between muscle and liver (Fig. 2). For δ^{202}Hg values the difference was less striking. A significant statistical difference was found only in BS fish (Fig. 2a); nevertheless, MDF was higher in muscle than liver for all sites. This result suggests that MeHg demethylation might indeed be occurring in the livers of European seabass. This is the first evidence that such a process might occur in this fish species, and specifically in juvenile individuals. This represents a very important result, considering existing conflicting literatures about MeHg demethylation capacity in fish organisms.

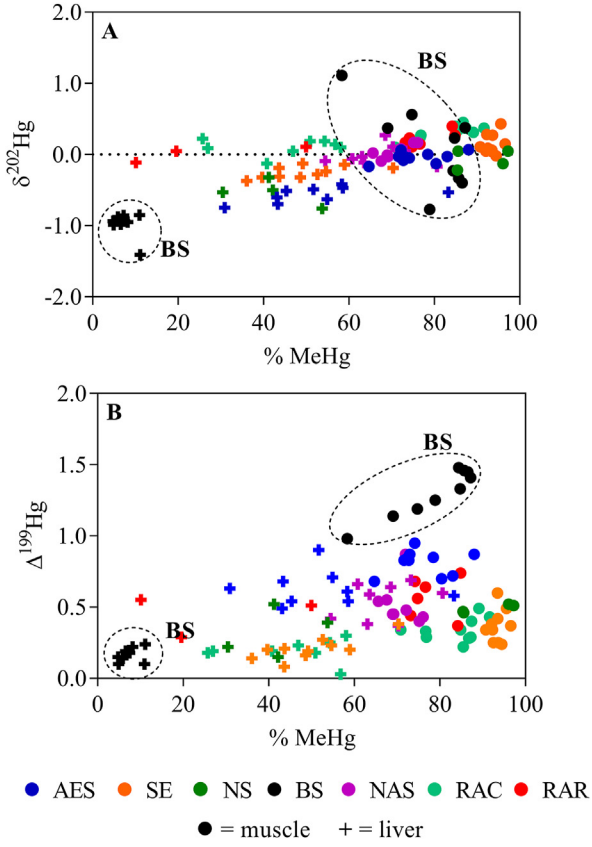

Fig. 2. δ^{202}Hg (**A**) and Δ^{199}Hg (**B**) values *vs.* % MeHg for all sampling sites of muscle and liver tissue. AES = Aegean Sea (blue), NS = North Sea (Green), SE = Seine Estuary (Orange), BS = Black Sea (Black), NAS = North Adriatic Sea (NAS), RAR = Ria d'Aveiro Reference (Red) and RAC = Ria d'Aveiro Contaminated (Light blue). The dotted ellipse is a figurative grouping of BS seabass. Muscle values are represented by the circle, and liver values by the cross. (For interpretation of the references to colour in this figure legend, the reader is referred to the Web version of this article.)

Regarding the hypothesis that *in vivo* demethylation was the only process affecting MDF in seabass, we should expect to have the

same δ^{202}Hg difference between muscle and liver across all sites. However, this was not the case since BS seabass presented a much larger δ^{202}Hg difference than the other sites. Cransveld et al. (2017) proposed that the particular Hg isotopic composition of the BS subpopulation could be explained by the presence of MeHg demethylation (Cransveld et al., 2017). Our findings have shown that such a process is occurring in all the sampled seabass. Therefore, one possibility is that BS seabass might demethylate MeHg at higher rates, which would lead to a larger difference in δ^{202}Hg values between muscle and liver. Several processes might determine higher raters of Hg organotropism and demethylation: the levels of local Hg pollution, fish age, exposure to different sources of Hg from the environment, fish diet, and finally the particular biogeochemistry of the studied area, which affects local Hg cycling in the marine environment. These factors will be analyzed one-by-one in the following paragraphs.

4.2. A higher extent of local Hg pollution hides inter-organ Hg MDF

Previous studies have shown that in highly polluted systems, liver can accumulate iHg directly from the environment, through the gills or the skin (Feng et al., 2015). For this reason, hepatic Hg levels and detoxification rates might be affected by levels of Hg pollution in the environment (Guilherme et al., 2008). Indeed, in areas with higher anthropogenic pollution discharge, studies have demonstrated a decrease in %MeHg in fish liver (Rua-Ibarz et al., 2019). This seems to be primarily due to two different processes: first, the exposure to higher levels of environmental iHg deriving from anthropogenic activities leads to higher accumulation of this Hg species in the liver (Gentès et al., 2015); secondly, the higher Hg intake in the animal (through diet or gills) leads to higher hepatic MeHg demethylation rates (Cizdziel et al., 2003; Perrot et al., 2015). If this were true, we would observe a larger difference in %MeHg between muscle and liver tissues in highly polluted areas compared to unpolluted ones. In the same way, because of the depletion in ^{202}Hg observed during demethylation of MeHg in liver, we should get a higher difference between muscle δ^{202}Hg and liver δ^{202}Hg in seabass collected in highly polluted areas.

In our study, the profile of %MeHg in the liver of European seabass indeed reflects the history of Hg contamination between our sampling sites, with moderately polluted areas such as NS and SE presenting ≈70% of MeHg in liver and the highly polluted ones like RAC and NAS presenting ≈40% of MeHg. The Ria d'Aveiro (RAC) has been subjected to Hg effluents from a chlor-alkali plant for almost five decades (1950–1994). Today, very high Hg concentrations can still be found in bottom sediments (Coelho et al., 2005; Mieiro et al., 2011). NAS samples were collected in the lagoon of Marano and Grado in the Gulf of Trieste. This area is known to have a long history of Hg pollution, due to the presence of the Idrija mercury mine and chlor-alkali plants active between 1949 and 1984 (Foucher et al., 2009; Živković et al., 2017). On the other hand, AES samples were collected in the Agiasma lagoon, which is today a RAMSAR protected area (Table 1). This region is usually associated with quite low levels of Hg (Christophoridis et al., 2007). This second result suggests that mercury accumulation and organotropism in European seabass from NAS, NS, SE, AES, RAR and RAC is governed by the extent of local pollution, and controlled by the protective role played by the liver. However, this cannot apply to BS, which contrasted with all other sites, showing the lowest THg levels and %MeHg in liver (around 7%, Table 2). Moreover, the difference between δ^{202}Hg in muscle and liver was found to be the greatest in BS fish, followed by the second least polluted site of AES. Conversely, the moderately and highly polluted areas did not show any significant differences (Figure S4). This result is in contrast with our previous observation of larger inter-organ MDF in more polluted areas, supporting the idea that the larger extent of BS MeHg hepatic demethylation is not governed by Hg pollution.

A possible factor influencing the rate of MeHg demethylation, and therefore Hg MDF, is fish age. BS seabass were one year old, while in NAS, SE, NS and AES we sampled two- and three-year-old fish (Cransveld et al., 2017). Several studies have demonstrated how the detoxifying activity of liver can change during the lifetime of an organism, due to metabolic shifts linked with growth rates (Le Croizier et al., 2020). Younger fast-growing animals have higher metabolic rates, which lead to faster isotopic routing and contaminant accumulation (Pinzone et al., 2017). Therefore, the large δ^{202}Hg tissue offset in BS might be due to the fact that these fish are younger than SE, NS, AES and NAS ones. However, this does not apply to RAC and RAR fish, which are also one year old, but do not show the same large δ^{202}Hg offset between tissues (Figure S4).

The similar age of NAS or RAC and BS fish therefore excludes attributing the difference in the extent of MeHg demethylation to growing rates. This, in addition to the inconsistency of BS seabass presenting both the highest inter-organ MDF and lowest Hg pollution, shows that while the levels of environmental Hg pollution generally influence Hg organotropism in this species, the inter-organ Hg MDF variability might not result from a difference in demethylation rates across sites.

It could instead be proposed that the Hg isotopic variability observed in our seven seabass subpopulations results from the extreme difference in Hg levels between the most polluted sites NAS and RAC and the least polluted sites of BS and AES. Indeed, in very contaminated areas, seabass might be exposed to levels of dietary MeHg so elevated that it can saturate the organism (Feng et al., 2015). In this situation, differences in Hg levels and isotopic values between organs might be masked (Havelková et al., 2008). This could be the reason for the absence of inter-organ MDF offset in seabass from NAS or RAC. On the other hand, we can readily discriminate Hg inter-organ transfer and demethylation processes in BS seabass because of the limited Hg pollution in the area.

4.3. Δ^{199}Hg MIF inter-tissue comparison indicates same Hg origin for all seabass populations

If Hg pollution was the only factor influencing seabass Hg isotopic composition, we would observe the same pattern in both AES and BS, because of their similar Hg levels. However, it is worth remembering that BS seabass were the only ones in which the δ^{202}Hg offset between the muscle and liver was significantly different. When comparing BS fish with the rest of the sampling sites, we can observe that the large difference in δ^{202}Hg is caused by significantly lower values (≈-1‰) in liver tissue compared to the other regions (Fig. 2a). Muscle δ^{202}Hg values are instead similar to other regions, in accordance with previous findings in estuarine biota (Kwon et al., 2014b). Beside metabolic processes, Hg stable isotope MDF can occur during a variety of biotic and dark abiotic reactions, such as microbial reduction of iHg (δ^{202}Hg ≈ −1.6‰) or microbial demethylation of MeHg (δ^{202}Hg ≈ −0.4‰) (Tsui et al., 2019). Therefore, the negative MDF signature of BS fish could reflect the local marine Hg biochemical cycle. However, the great variability of processes causing MDF complicates the interpretation of our data.

Hg stable isotope MIF is caused by photochemical processes in the environment and is not modified by *in vivo* metabolism (Blum et al., 2014). For this reason, it can be used more easily to trace Hg sources in marine fish (Zheng and Hintelmann, 2009). Δ^{199}Hg values should not differ between muscle and liver tissues when fish are exposed to Hg originating from a single source point (Perrot

et al., 2010). As expected, we found no statistical difference between liver and muscle Δ^{199}Hg values from all sites, again with the single exception of BS, whose muscle Δ^{199}Hg values were >1‰ higher than those for liver (Fig. 2b). These values are also higher than Δ^{199}Hg found in all the other sites. As for δ^{202}Hg values, BS MIF signature was the only one to correlate positively with %MeHg between tissues, confirming again that both MDF and MIF in this population depends on Hg species distribution between muscle and liver.

A first hypothesis is that the two tissues represent two separate endmembers of Hg in this population. In fish, the liver accumulates Hg in three forms: MeHg from the diet, iHg from demethylated MeHg, and environmental iHg. While more than 95% of assimilated dietary MeHg is absorbed and mostly stored in muscle (Maury-Brachet et al., 2006), only 10% of iHg remains in the organism (Gentès et al., 2015). For this reason, we usually find very low levels of iHg (Wang and Wong, 2003). In the presence of a local point source of iHg, however, this form can accumulate at higher rates in both liver and muscle tissue (Feng et al., 2015).

The majority of Hg accumulated in BS liver is in an inorganic form (≈90%, Fig. 3). Thus, the near-zero Δ^{199}Hg values presented by BS seabass liver could reflect the isotopic composition of iHg accumulated directly from the environment (Fig. 3b). On the other hand, BS muscle presents both Hg species, with a majority of MeHg (60–90%). In that case, Δ^{199}Hg values in this tissue could represent a mix of multiple sources. Δ^{199}Hg values around 1.5‰ could represent MeHg coming from the diet, whilst lower MIF could be linked to the remaining 10–40% of iHg. This is confirmed by the positive correlation between Δ^{199}Hg values and %MeHg in muscle (Fig. 3b).

Inorganic Hg coming from industrial sources can have near-zero Δ^{199}Hg, while watershed loading can even impart negative MIF (Du et al., 2018; Lepak et al., 2015). Therefore, one possibility for the low hepatic MIF might be that Hg stored in BS seabass liver comes from a local point source of industrial origin (Wiederhold et al., 2015). The BS samples were taken along the northern Turkish coast, between the Sinop peninsula and the Kızılırmak estuary. This area is known for heavy industrial activity and the input of totally unregulated and uncontrolled drainage water from upriver mining and agricultural areas (Bat et al., 2010; Gökkurt et al., 2007). However, recent literature has shown that the amount of freshwater discharge of particulate Hg in this locality, and its bioaccumulation in marine biota, is negligible compared to other trace elements (e.g. < 50 ng g^{-1} ww in fish liver, < DL in invertebrates) (Bat et al., 2018, 2019). Therefore, our Black Sea sampling site can be considered as a relatively unpolluted area with regards to Hg (Table 1), excluding the hypothesis of a particular point source of anthropogenic origin. Additionally, in Fig. 1b we can see how the values of the Δ^{199}Hg/Δ^{201}Hg slopes for both liver (1.69 ± 0.03) and muscle (1.26 ± 0.02) confirm that all Hg accumulated in BS seabass derives from photo-demethylated MeHg in the water column, in the same way as the other regions. This combination of evidence excludes our hypothesis of the presence of an additional source of iHg in the Black Sea population.

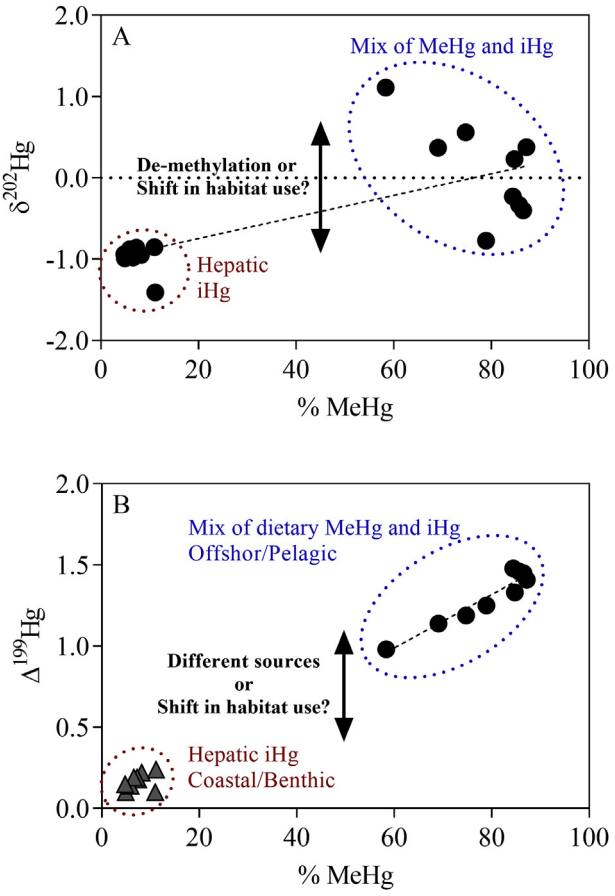

Fig. 3. δ^{202}Hg *vs.* MeHg **(A)** and Δ^{199}Hg *vs.* MeHg **(B)** in muscle (black dots) and liver (grey triangles) of the Black sea population of seabass *D. labrax*. MDF and MIF signatures are shown in per mill (‰), while MeHg proportion is represented in percentage (%). Significant correlation is represented by a discontinuous regression line.

4.4. Δ^{199}Hg MIF of uncontaminated Black Sea waters show short-term ontogenetic shifts in fish

Because of their different metabolic roles, muscle and liver tissues integrate different time periods of the fish life cycle, and therefore also their habitat use and Hg exposure levels (Madigan et al., 2012). One of the biggest complications in the interpretation of these kinds of results is that isotopic and elemental uptake and excretion can occur at very different rates (Carter et al., 2019). To our knowledge, there is no information about isotopic routing in fish liver yet. However, if we consider that this is an organism where dietary MeHg is quickly metabolized and accumulated as inert iHg with time, it is safe to accept that, as for mammals and birds, it might integrate the entire life of the fish. MeHg half-life in fish muscle is much shorter, around two years (Kwon et al., 2016; Tollefson and Cordle, 1986). Therefore, we could propose that liver of BS seabass integrates information about Hg exposure during the entire life of the fish, while muscle does so only for the last year. If this were the case, we could hypothesize that the large MDF and MIF offsets between muscle and liver are showing two separated temporal snapshots of the first year of life of BS seabass.

The seabass is a bentho-pelagic species which undergoes seasonal migrations between their feeding (offshore) and spawning (estuaries) areas (Pawson et al., 1987). From birth until their first year, immature fish inhabit their nursery areas (e.g. lagoons, estuaries) (López et al., 2015). In some regions juvenile seabass can already start exploring offshore waters during their first summer, but they never venture into deeper waters until they reach sexual maturity (around five years of age) (Jennings et al., 1991).

Hepatic near-zero MIF and negative MDF of BS fish denote a coastal and benthic habitat use, in accordance with previous literature about the trophic ecology of estuarine fish (Kwon et al., 2014b; Li et al., 2016; Senn et al., 2010). In these areas, most Hg accumulated in fish derives from MeHg formed in sediments (Li et al., 2016). The low MDF and MIF values are a consequence of the reduced amount of photochemical degradation due to the

presence of more suspended particle loads and DOC concentrations that reduce light penetration (Kwon et al., 2014b).

On the other hand, in marine offshore and pelagic food webs, MeHg derives mostly from wet precipitation (Δ^{199}Hg = −1 to 1‰) or deposition of gaseous elemental Hg (Δ^{199}Hg = 0.5‰−1‰) (Kwon et al., 2020). This results in the high MIF values found in BS seabass muscle (Fig. 3b). Therefore, our findings suggest that in BS seabass, hepatic MIF, mostly related to the iHg fraction, would represent the period of their life spent in the estuaries feeding upon benthic invertebrates in the sediments. On the other hand, muscle—and the isotopic composition related to MeHg—might show a more recent signature, corresponding to the first exploratory trips to pelagic waters.

Cransveld et al. (2017) have thoroughly discussed the impact of seabass diet on MeHg accumulation and Hg MDF and MIF values, integrating fish stomach content analysis with the measurement of nitrogen and carbon stable isotope ratios (δ^{15}N and δ^{13}C, respectively). Although they found a difference in fish trophic level (TL, calculated from δ^{15}N values) and δ^{13}C values, they did not find any correlation with seabass THg or MeHg concentrations (Cransveld et al., 2017). Stomach content revealed a similar variety of prey across all sites, confirming the largely opportunistic feeding behavior of seabass (Cransveld et al., 2017). This further confirms that the differences in inter-organ MDF and MIF in BS fish, as well as the other sites, depend more on shifts in habitat use than on diet.

Finally, while the very low contamination levels of the BS site allow the net differentiation of local seabass from the other regions with regards to inter-tissue fractionation, it also separates this subpopulation for the large heterogeneity of muscle MDF and MIF values (Fig. 2). This is linked with the unique oceanographic features of the Black Sea (e.g. low salinity, strong freshwater input, semi-permanent stratification, etc.) (Bakan and Büyükgüngör, 2000; Capet et al., 2016; Özsoy and Ünlüata, 1997). These features lengthen marine Hg processing and recycling between water layers, resulting in higher and more diverse Δ^{199}Hg and δ^{202}Hg values (Blum et al., 2013; Motta et al., 2019).

Our findings underline the necessity of collecting detailed information about the history of Hg pollution, and its cycling and sourcing in the environment, before studying its accumulation, organotropism and transformation within marine predatory fish through the analysis of Hg stable isotope ratios.

5. Conclusion

The main findings of this study can be summarized as follows:

1. The multi-tissue comparison of Hg MDF and MIF signals produced evidence of MeHg demethylation in the liver of a fish species, as well as trace Hg accumulation dynamics between different populations of a marine predator;
2. In general, the levels of environmental Hg pollution influence Hg organotropism and apparently also the extent of hepatic demethylation in marine predatory fish. However, it is not the only factor contributing to Hg isotopic variability in the European seabass;
3. In highly contaminated areas, inter-organ MDF might get hindered by Hg saturation in fish tissues. This has to be taken into account in the interpretation of Hg stable isotopes in further studies. On the other hand, in uncontaminated sites (<200 ng g^{-1} dw in fish) such as the Black Sea, the inter-organ Hg MDF and MIF can trace short-term shifts in fish habitat use;
4. Additionally, the particular oceanographic features of the Black Sea basin influence Hg cycling and processing in the water column, as highlighted by BS seabass Δ^{199}Hg and δ^{202}Hg values.

Authors statement

Marianna Pinzone: Data curation, Writing − review and editing, Visualization, Formal analysis, Conceptualization. Alice Cransveld: Conceptualization, Methodology, Formal analysis, Writing − original draft. Emmanuel Tessier: Analytical measurements, Software, Validation. Sylvain Bérail: Resources, Analytical measurements, Validation. Joseph Schnitzler: Supervision, Formal analysis, Validation. Krishna Das: Resources, Project administration, Funding acquisition, Supervision. David Amouroux: Resources, Supervision, Validation.

Main finding

Our novel results support the occurrence of *in vivo* MeHg demethylation in European seabass. They also show that, in this fish, environmental levels of Hg pollution influence demethylation rates and inter-organ MDF.

Declaration of competing interest

The authors declare that they have no known competing financial interests or personal relationships that could have appeared to influence the work reported in this paper.

Acknowledgments

Alice Cransveld and Marianna Pinzone acknowledge a PhD F.R.I.A. grant (F.R.S-FNRS). Krishna Das is a Senior F.R.S.-FNRS Research Associate (Fond pour la Recherche Scientifique). The authors thank Emmanuil Koutrakis (Fisheries Research Institute, Hellenic Agricultural Organisation, Greece), Ayaka Ozturk (Faculty of Fisheries, Istanbul University, Turkey), Nicola Bettoso (Agenzia Regionale per la Protezione dell'Ambiente del Friuli Venezia Giulia [ARPA FVG], Italy) and Cláudia Mieiro (CESAM and Departamento de Biologia, Universidade de Aveiro, Portugal) for their help in sampling the seabass. The authors thank the members of the LCABIE, and the IPREM institute from Pau University for their warm welcome and for sharing their knowledge and expertise with us. Special thanks to Julien Barre for his constant help and guidance in the laboratory, and to Caiyan Feng for her practical assistance in some GC-ICP-MS analysis. English proofing was conducted by the Skylark Academic & Book Editing service (Invoice N° 427). The authors would like to pay tribute to the memory of the late Mr. Renzo Biondo for his support in laboratory analyses.

Appendix A. Supplementary data

Supplementary data to this article can be found online at https://doi.org/10.1016/j.envpol.2021.117008.

References

Bakan, G., Büyükgüngör, H., 2000. The Black sea. Mar. Pollut. Bull. 41, 24−43. https://doi.org/10.1016/S0025-326X(00)00100-4.

Bat, L., Gökkurt, O., Sezgin, M., Üstün, F., Sahin, F., 2010. Evaluation of the Black sea land based sources of pollution the coastal region of Turkey. Open Mar. Biol. J. 3, 112−124. https://doi.org/10.2174/1874450800903010112.

Bat, L., Şahin, F., Öztekin, A., 2019. Metal bioaccumulation of Mytilaster lineatus (gmelin, 1791) collected from Sinop coast in the southern Black sea. Eur. J. Biol. 78, 23−28. https://doi.org/10.26650/eurjbiol.2019.0001.

Bat, L., Sezgin, M., Sahin, F., 2018. Heavy metal contamination of aquatic resources from Turkish Black Sea waters. J. Environ. Prot. Ecol. 19, 558−563.

Bergquist, B.A., Blum, J.D., 2009. The odds and evens of mercury isotopes: applications of mass-dependent and mass-independent isotope fractionation. Elements 5, 353−357. https://doi.org/10.2113/gselements.5.6.353.

Bergquist, B.A., Blum, J.D., 2007. Mass-dependent and -independent fractionation of hg isotopes by photoreduction in aquatic systems. Science 84 318, 417−420.

https://doi.org/10.1126/science.1148050.
Blum, J.D., Popp, B.N., Drazen, J.C., Anela Choy, C., Johnson, M.W., 2013. Methylmercury production below the mixed layer in the north pacific ocean. Nat. Geosci. 6, 879–884. https://doi.org/10.1038/ngeo1918.
Blum, J.D., Sherman, L.S., Johnson, M.W., 2014. Mercury isotopes in earth and environmental sciences. Annu. Rev. Earth Planet Sci. 42, 249–269. https://doi.org/10.1146/annurev-earth-050212-124107.
Booth, S., Zeller, D., 2005. Mercury, food webs, and marine mammals: implications of diet and climate change for human health. Environ. Health Perspect. 113, 521–526.
Bystrom, E., 2008. Assessment of Mercury Methylation and Demethylation with Focus on Chemical Speciation and Biological Processes. Georgia Institute of Technology.
Capet, A., Stanev, E.V., Beckers, J.M., Murray, J.W., Grégoire, M., 2016. Decline of the Black sea oxygen inventory. Biogeosciences 13, 1287–1297. https://doi.org/10.5194/bg-13-1287-2016.
Carter, W.A., Bauchinger, U., McWilliams, S.R., 2019. The importance of isotopic turnover for understanding key aspects of animal ecology and nutrition. Diversity 11. https://doi.org/10.3390/D11050084.
Chandan, P., Ghosh, S., Bergquist, B.A., 2015. Mercury isotope fractionation during aqueous photoreduction of monomethylmercury in the presence of dissolved organic matter. Environ. Sci. Technol. 49, 259–267. https://doi.org/10.1021/es5034553.
Christophoridis, A., Stamatis, N., Orfanidis, S., 2007. Sediment heavy metals of a mediterranean coastal lagoon: Agiasma, nestos delta, eastern Macedonia (Greece). Transitional Waters Bull 1, 33–43. https://doi.org/10.1285/i1825229Xv1n4p33.
Cizdziel, J., Hinners, T., Cross, C., Pollard, J., 2003. Distribution of mercury in the tissues of five species of freshwater fish from Lake Mead, USA. J. Environ. Monit. 5, 802–807. https://doi.org/10.1039/b307641p.
Coelho, J.P., Pereira, M.E., Duarte, A., Pardal, M.A., 2005. Macroalgae response to a mercury contamination gradient in a temperate coastal lagoon (Ria de Aveiro, Portugal). Estuar. Coast Shelf Sci. 65, 492–500. https://doi.org/10.1016/j.ecss.2005.06.020.
Cransveld, A., Amouroux, D., Tessier, E., Koutrakis, E., Ozturk, A.A., Bettoso, N., Mieiro, C.L., Bérail, S., Barre, J.P.G., Sturaro, N., Schnitzler, J., Das, K., 2017. Mercury stable isotopes discriminate different populations of European seabass and trace potential Hg sources around Europe. Environ. Sci. Technol. 51, 12219–12228. https://doi.org/10.1021/acs.est.7b01307.
Du, B., Feng, X., Li, P., Yin, R., Yu, B., Sonke, J.E., Guinot, B., Anderson, C.W.N., Maurice, L., 2018. Use of mercury isotopes to quantify mercury exposure sources in inland populations, China. Environ. Sci. Technol. 52, 5407–5416. https://doi.org/10.1021/acs.est.7b05638.
Du, H., Ma, M., Igarashi, Y., Wang, D., 2019. Biotic and abiotic degradation of methylmercury in aquatic ecosystems: a review. Bull. Environ. Contam. Toxicol. 102, 605–611. https://doi.org/10.1007/s00128-018-2530-2.
Eagles-Smith, C.A., Ackerman, J.T., Yee, J., Adelsbach, T.L., 2009. Mercury demethylation in waterbird livers: dose-response thresholds and differences among species. Environ. Toxicol. Chem. 28, 568–577. https://doi.org/10.1897/08-245.1.
Feng, C., Pedrero, Z., Gentès, S., Barre, J., Renedo, M., Tessier, E., Berail, S., Maury-Brachet, R., Mesmer-Dudons, N., Baudrimont, M., Legeay, A., Maurice, L., Gonzalez, P., Amouroux, D., 2015. Specific pathways of dietary methylmercury and inorganic mercury determined by mercury speciation and isotopic composition in zebrafish (Danio rerio). Environ. Sci. Technol. 49, 12984–12993. https://doi.org/10.1021/acs.est.5b03587.
Foucher, D., Ogrinc, Hintelmann, H., 2009. Tracing mercury contamination from the Idrija mining region (Slovenia) to the Gulf of trieste using Hg isotope ratio measurements. Environ. Sci. Technol. 43, 33–39. https://doi.org/10.1021/es801772b.
Gantner, N., Hintelmann, H., Zheng, W., Muir, D.C., 2009. Variations in stable isotope fractionation of Hg in food webs of Arctic lakes. Environ. Sci. Technol. 43, 9148–9154. https://doi.org/10.1021/es901771r.
Gehrke, G.E., Blum, J.D., Slotton, D.G., Greenfield, B.K., 2011. Mercury isotopes link mercury in san francisco bay forage fish to surface sediments. Environ. Sci. Technol. 45, 1264–1270. https://doi.org/10.1021/es103053y.
Gentès, S., Maury-Brachet, R., Feng, C., Pedrero, Z., Tessier, E., Legeay, A., Mesmer-Dudons, N., Baudrimont, M., Maurice, L., Amouroux, D., Gonzalez, P., 2015. Specific effects of dietary methylmercury and inorganic mercury in zebrafish (Danio rerio) determined by genetic, histological, and metallothionein responses. Environ. Sci. Technol. 49, 14560–14569. https://doi.org/10.1021/acs.est.5b03586.
Gökkurt, O., Bat, L., Sahin, F., 2007. The investigation of some physicochemical parameters in the Middle Black Sea (Sinop. Turkey). In: Proceedings of 7th National Environmental Engineering Congress, pp. 869–873.
Gonzalez, P., Dominique, Y., Massabuau, J.C., Boudou, A., Bourdineaud, J.P., 2005. Comparative effects of dietary methylmercury on gene expression in liver, skeletal muscle, and brain of the zebrafish (Danio rerio). Environ. Sci. Technol. 39, 3972–3980. https://doi.org/10.1021/es0483490.
Gratz, L.E., Keeler, G.J., Blum, J.D., Sherman, L.S., 2010. Isotopic composition and fractionation of mercury in Great Lakes precipitation and ambient air. Environ. Sci. Technol. 44, 7764–7770. https://doi.org/10.1021/es100383w.
Guilherme, S., Válega, M., Pereira, M.E., Santos, M.A., Pacheco, M., 2008. Antioxidant and biotransformation responses in Liza aurata under environmental mercury exposure - relationship with mercury accumulation and implications for public health. Mar. Pollut. Bull. 56, 845–859. https://doi.org/10.1016/j.marpolbul.2008.02.003.
Gworek, B., Bemowska-Kałabun, O., Kijeńska, M., Wrzosek-Jakubowska, J., 2016. Mercury in marine and oceanic waters—a review. Water Air Soil Pollut. 227 https://doi.org/10.1007/s11270-016-3060-3.
Habran, S., Crocker, D.E., Debier, C., Das, K., 2012. How are trace elements mobilized during the postweaning fast in Northern elephant seals? Environ. Toxicol. Chem. 31, 2354–2365. https://doi.org/10.1002/etc.1960.
Havelková, M., Dušek, L., Némethová, D., Poleszczuk, G., Svobodová, Z., 2008. Comparison of mercury distribution between liver and muscle - a biomonitoring of fish from lightly and heavily contaminated localities. Sensors 8, 4095–4109. https://doi.org/10.3390/s8074095.
Hong, Y.-S., Kim, Y.-M., Lee, K.-E., 2012. Methylmercury exposure and health effects. J. Prev. Med. public Health 45, 353–363. https://doi.org/10.3961/jpmph.2012.45.6.353.
Jardine, T., Kidd, K.A., Fisk, A.T., 2006. Critical review applications , considerations , and sources of uncertainty when using stable isotope analysis in ecotoxicology. Crit. Rev. 40, 7501–7511. https://doi.org/10.1021/es061263h.
Jennings, S., Lancaster, J.E., Ryland, J.S., Shackley, S.E., 1991. The age structure and growth dynamics of young-of-the-year bass, dicentrarchus labrax, populations. J. Mar. Biol. Assoc. U. K. 71, 799–810. https://doi.org/10.1017/S0025315400053467.
Kritee, K., Motta, L.C., Blum, J.D., Tsui, M.T.K., Reinfelder, J.R., 2018. Photomicrobial visible light-induced magnetic mass independent fractionation of mercury in a marine microalga. ACS Earth Sp. Chem. 2, 432–440. https://doi.org/10.1021/acsearthspacechem.7b00056.
Kwon, S.Y., Blum, J.D., Carvan, M.J., Basu, N., Head, J.A., Madenjian, C.P., David, S.R., 2012. Absence of fractionation of mercury isotopes during trophic transfer of methylmercury to freshwater fish in captivity. Environ. Sci. Technol. 46, 7527–7534. https://doi.org/10.1021/es300794q.
Kwon, S.Y., Blum, J.D., Chen, C.Y., Meattey, D.E., Mason, R.P., 2014a. Mercury isotope study of sources and exposure pathways of methylmercury in estuarine food webs in the northeastern U.S. Environ. Sci. Technol. 48, 10089–10097. https://doi.org/10.1021/es5020554.
Kwon, S.Y., Blum, J.D., Chen, C.Y., Meattey, D.E., Mason, R.P., 2014b. Mercury isotope study of sources and exposure pathways of methylmercury in estuarine food webs in the northeastern U.S. Environ. Sci. Technol. 48, 10089–10097. https://doi.org/10.1021/es5020554.
Kwon, S.Y., Blum, J.D., Madigan, D.J., Block, B.A., Popp, B.N., 2016. Quantifying mercury isotope dynamics in captive Pacific bluefin tuna (Thunnus orientalis). Elem. Sci. Anthr. 4, 000088 https://doi.org/10.12952/journal.elementa.000088.
Kwon, S.Y., Blum, J.D., Yin, R., Tsui, M.T.K., Yang, Y.H., Choi, J.W., 2020. Mercury stable isotopes for monitoring the effectiveness of the Minamata Convention on Mercury. Earth Sci. Rev. 203, 103111. https://doi.org/10.1016/j.earscirev.2020.103111.
Lang, T., Kruse, R., Haarich, M., Wosniok, W., 2017. Mercury species in dab (Limanda limanda) from the North Sea, Baltic Sea and Icelandic waters in relation to host-specific variables. Mar. Environ. Res. 124, 32–40. https://doi.org/10.1016/j.marenvres.2016.03.001.
Le Croizier, G., Lorrain, A., Sonke, J.E., Jaquemet, S., Schaal, G., Renedo, M., Besnard, L., Cherel, Y., Point, D., 2020. Mercury isotopes as tracers of ecology and metabolism in two sympatric shark species. Environ. Pollut. 265 https://doi.org/10.1016/j.envpol.2020.114931.
Lehnherr, I., St Louis, V.L., 2009. Importance of ultraviolet radiation in the photodemethylation of methylmercury in freshwater ecosystems. Environ. Sci. Technol. 43, 5692–5698. https://doi.org/10.1021/es9002923.
Lepak, R.F., Yin, R., Krabbenhoft, D.P., Ogorek, J.M., Dewild, J.F., Holsen, T.M., Hurley, J.P., 2015. Use of stable isotope signatures to determine mercury sources in the great lakes. Environ. Sci. Technol. Lett. 2, 335–341. https://doi.org/10.1021/acs.estlett.5b00277.
Li, M., Juang, C.A., Ewald, J.D., Yin, R., Mikkelsen, B., Krabbenhoft, D.P., Balcom, P.H., Dassuncao, C., Sunderland, E.M., 2020. Selenium and stable mercury isotopes provide new insights into mercury toxicokinetics in pilot whales. Sci. Total Environ. 710, 136325. https://doi.org/10.1016/j.scitotenv.2019.136325.
Li, M., Schartup, A.T., Valberg, A.P., Ewald, J.D., Krabbenhoft, D.P., Yin, R., Balcom, P.H., Sunderland, E.M., 2016. Environmental origins of methylmercury accumulated in subarctic estuarine fish indicated by mercury stable isotopes. Environ. Sci. Technol. 50, 11559–11568. https://doi.org/10.1021/acs.est.6b03206.
López, R., De Pontual, H., Bertignac, M., Mahévas, S., 2015. What can exploratory modelling tell us about the ecobiology of European sea bass (Dicentrarchus labrax): a comprehensive overview. Aquat. Living Resour. 28, 61–79. https://doi.org/10.1051/alr/2015007.
Lu, X., Liu, Y., Johs, A., Zhao, L., Wang, T., Yang, Z., Lin, H., Elias, D.A., Pierce, E.M., Liang, L., Barkay, T., Gu, B., 2016. Anaerobic mercury methylation and demethylation by geobacter bemidjiensis bem. Environ. Sci. Technol. 50, 4366–4373. https://doi.org/10.1021/acs.est.6b00401.
Luo, H., Cheng, Q., Pan, X., 2020. Photochemical behaviors of mercury (Hg) species in aquatic systems: a systematic review on reaction process, mechanism, and influencing factor. Sci. Total Environ. 720, 137540. https://doi.org/10.1016/j.scitotenv.2020.137540.
Madigan, D.J., Litvin, S.Y., Popp, B.N., Carlisle, A.B., Farwell, C.J., Block, B.A., 2012. Tissue turnover rates and isotopic trophic discrimination factors in the endothermic teleost, pacific bluefin tuna (Thunnus orientalis). PloS One 7. https://doi.org/10.1371/journal.pone.0049220.
Man, Y., Yin, R., Cai, K., Qin, C., Wang, J., Yan, H., Li, M., 2019. Primary amino acids affect the distribution of methylmercury rather than inorganic mercury among

tissues of two farmed-raised fish species. Chemosphere 225, 320–328. https://doi.org/10.1016/j.chemosphere.2019.03.058.
Mason, R.P., Lawson, N.M., Sheu, G.R., 2001. Mercury in the atlantic ocean: factors controlling air-sea exchange of mercury and its distribution in the upper waters. Deep. Res. Part II Top. Stud. Oceanogr. 48, 2829–2853. https://doi.org/10.1016/S0967-0645(01)00020-0.
Maury-Brachet, R., Durrieu, G., Dominique, Y., Boudou, A., 2006. Mercury distribution in fish organs and food regimes: significant relationships from twelve species collected in French Guiana (Amazonian basin). Sci. Total Environ. 368, 262–270. https://doi.org/10.1016/j.scitotenv.2005.09.077.
Mieiro, C., Pacheco, M., Pereira, M., Duarte, A., 2011. Mercury organotropism in feral European sea bass (Dicentrarchus labrax). Arch. Environ. Contam. Toxicol. 61, 135–143. https://doi.org/10.1007/s00244-010-9591-5.
Mieiro, C.L., Pacheco, M., Pereira, M.E., Duarte, A.C., 2009. Mercury distribution in key tissues of fish (Liza aurata) inhabiting a contaminated estuary - implications for human and ecosystem health risk assessment. J. Environ. Monit. 11, 1004–1012. https://doi.org/10.1039/b821253h.
Motta, L.C., Blum, J.D., Johnson, M.W., Umhau, B.P., Popp, B.N., Washburn, S.J., Drazen, J.C., Benitez-Nelson, C.R., Hannides, C.C.S., Close, H.G., Lamborg, C.H., 2019. Mercury cycling in the north pacific subtropical gyre as revealed by mercury stable isotope ratios. Global Biogeochem. Cycles 33, 777–794. https://doi.org/10.1029/2018GB006057.
Mozaffarian, D., Rimm, E.B., 2008. Fish intake, contaminants, and human health evaluating the risks and the benefits. J. Am. Med. Assoc. 296, 1885–1899.
Obrist, D., Kirk, J.L., Zhang, L., Sunderland, E.M., Jiskra, M., Selin, N.E., 2018. A review of global environmental mercury processes in response to human and natural perturbations: changes of emissions, climate, and land use. Ambio 47, 116–140. https://doi.org/10.1007/s13280-017-1004-9.
Oliveira Ribeiro, C.A., Rouleau, C., Pelletier, É., Audet, C., Tjälve, H., 1999. Distribution kinetics of dietary methylmercury in the arctic charr (Salvelinus alpinus). Environ. Sci. Technol. 33, 902–907. https://doi.org/10.1021/es980242n.
Özsoy, E., Ünlüata, Ü., 1997. Oceanography of the Black Sea: a review of some recent results. Earth Sci. Rev. 42, 231–272. https://doi.org/10.1016/S0012-8252(97)81859-4.
Pawson, M.G., Pickett, G.D., Kelley, D.F., 1987. The distribution and migrations of bass, Dicentrarchus labrax L., in waters around England and Wales as shown by tagging. J. Mar. Biol. Assoc. U. K. 67, 183–217. https://doi.org/10.1017/S0025315400026448.
Pentreath, R.J., 1976. The accumulation of mercury from food by the plaice,< i> Pleuronectes platessa</i> L. J. Exp. Mar. Biol. Ecol. 25, 51–65.
Perga, M.E., Gerdeaux, D., 2005. 'Are fish what they eat' all year round? Oecologia 144, 598–606. https://doi.org/10.1007/s00442-005-0069-5.
Perrot, V., Epov, V.N., Pastukhov, M.V., Grebenshchikova, V.I., Zouiten, C., Sonke, J.E., Husted, S., Donard, O.F.X., Amouroux, D., 2010. Tracing sources and bioaccumulation of mercury in fish of lake Baikal– angara river using Hg isotopic composition. Environ. Sci. Technol. 44, 8030–8037. https://doi.org/10.1021/es101898e.
Perrot, V., Masbou, J., Pastukhov, M.V., Epov, V.N., Point, D., Bérail, S., Becker, P.R., Sonke, J.E., Amouroux, D., 2015. Natural Hg isotopic composition of different Hg compounds in mammal tissues as a proxy for in vivo breakdown of toxic methylmercury. Metallomics 8, 170–178. https://doi.org/10.1039/c5mt00286a.
Pinzone, M., Acquarone, M., Huyghebaert, L., Sturaro, N., Michel, L.N., Siebert, U., Das, K., 2017. Carbon, nitrogen and sulphur isotopic fractionation in captive juvenile hooded seal (Cystophora cristata): application for diet analysis. Rapid Commun. Mass Spectrom. 31 https://doi.org/10.1002/rcm.7955.
Point, D., Sonke, J.E., Day, R.D., Roseneau, D.G., Hobson, K.A., Pol, S.S. Vander, Moors, A.J., Pugh, R.S., Donard, O.F.X., Becker, P.R., 2011. Methylmercury photodegradation influenced by sea-ice cover in Arctic marine ecosystems. Nat. Geosci. 4, 188–194. https://doi.org/10.1038/ngeo1049.
Regnell, O., Watras, C.J., 2019. Microbial mercury methylation in aquatic environments: a critical review of published field and laboratory studies. Environ. Sci. Technol. 53, 4–19. https://doi.org/10.1021/acs.est.8b02709.
Renedo, M., Amouroux, D., Duval, B., Carravieri, A., Tessier, E., Barre, J., Bérail, S., Pedrero, Z., Cherel, Y., Bustamante, P., 2018. Seabird tissues as efficient biomonitoring tools for Hg isotopic investigations: implications of using blood and feathers from chicks and adults. Environ. Sci. Technol. 52, 4227–4234. https://doi.org/10.1021/acs.est.8b00422.
Renedo, M., Pedrero, Z., Amouroux, D., Cherel, Y., Bustamante, P., 2021. Mercury isotopes of key tissues document mercury metabolic processes in seabirds. Chemosphere 263, 127777. https://doi.org/10.1016/j.chemosphere.2020.127777.
Renzoni, A., Zino, F., Franchi, E., 1998. Mercury levels along the food chain and risk for exposed populations. Environ. Res. 77, 68–72. https://doi.org/10.1006/enrs.1998.3832.
Rodríguez Martín-Doimeadios, R.C., Krupp, E., Amouroux, D., Donard, O.F.X., 2002. Application of isotopically labeled methylmercury for isotope dilution analysis of biological samples using gas chromatography/ICPMS. Anal. Chem. 74, 2505–2512. https://doi.org/10.1021/ac011157s.
Rua-Ibarz, A., Bolea-Fernandez, E., Maage, A., Frantzen, S., Sanden, M., Vanhaecke, F., 2019. Tracing mercury pollution along the Norwegian coast via elemental, speciation, and isotopic analysis of liver and muscle tissue of deep-water marine fish (brosme brosme). Environ. Sci. Technol. 53, 1776–1785. https://doi.org/10.1021/acs.est.8b04706.
Senn, D.B., Chesney, E.J., Blum, J.D., Bank, M.S., Maage, A., Shine, J.P., 2010. Stable isotope (N, C, Hg) study of methylmercury sources and trophic transfer in the Northern Gulf of Mexico. Environ. Sci. Technol. 44, 1630–1637.
Serrell, N., Chen, C.Y., Lambert, K.F., Driscoll, C.T., Mason, R.P., Sunderland, E.M., Rardin, L.R., 2012. Marine mercury fate: from sources to seafood consumers. Environ. Res. 119, 1–2. https://doi.org/10.1016/j.envres.2012.10.001.
Sherman, L.S., Blum, J.D., 2013. Mercury stable isotopes in sediments and largemouth bass from Florida lakes, USA. Sci. Total Environ. 448, 163–175. https://doi.org/10.1016/j.scitotenv.2012.09.038.
Sherman, L.S., Blum, J.D., Johnson, K.P., Keeler, G.J., Barres, J.A., Douglas, T.A., 2010. Mass-independent fractionation of mercury isotopes in Arctic snow driven by sunlight. Nat. Geosci. 3, 173–177. https://doi.org/10.1038/ngeo758.
Sonke, J.E., Heimbürger, L.E., Dommergue, A., 2013. Mercury biogeochemistry: paradigm shifts, outstanding issues and research needs. Compt. Rendus Geosci. 345, 213–224. https://doi.org/10.1016/j.crte.2013.05.002.
Sonne, C., Aspholm, O., Dietz, R., Andersen, S., Berntssen, M.H.G., Hylland, K., 2009. A study of metal concentrations and metallothionein binding capacity in liver, kidney and brain tissues of three Arctic seal species. Sci. Total Environ. 407, 6166–6172. https://doi.org/10.1016/j.scitotenv.2009.08.029.
Sunderland, E.M., Dalziel, J., Heyes, A., Branfireun, B.A., Krabbenhoft, D.P., Gobas, F.A.P.C., 2010. Response of a macrotidal estuary to changes in anthropogenic mercury loading between 1850 and 2000. Environ. Sci. Technol. 44, 1698–1704. https://doi.org/10.1021/es9032524.
Tollefson, L., Cordle, F., 1986. Methylmercury in fish: a review of residue levels, fish consumption and regulatory action in the United States. Environ. Health Perspect. 68, 203–208. https://doi.org/10.1289/ehp.8668203.
Tsui, M.T.K., Blum, J.D., Kwon, S.Y., 2019. Review of stable mercury isotopes in ecology and biogeochemistry. Sci. Total Environ. 135386 https://doi.org/10.1016/j.scitotenv.2019.135386.
UNEP, 2018. Global Mercury Assessment 2018 270.
UNEP, 2013. Global Mercury Assessment 2013: Sources, Emissions, Releases and Environmental Transport. United Nation Environment Programme Chemical Branch, Geneva, Switzerland.
Wagemann, R., Trebacz, E., Boila, G., Lockhart, W.L., 1998. Methylmercury and total mercury in tissues of arctic marine mammals. Sci. Total Environ. 218, 19–31.
Wang, R., Feng, X. Bin, Wang, W.X., 2013. In vivo mercury methylation and demethylation in freshwater tilapia quantified by mercury stable isotopes. Environ. Sci. Technol. 47, 7949–7957. https://doi.org/10.1021/es3043774.
Wang, W.X., Tan, Q.G., 2019. Applications of dynamic models in predicting the bioaccumulation, transport and toxicity of trace metals in aquatic organisms. Environ. Pollut. 252, 1561–1573. https://doi.org/10.1016/j.envpol.2019.06.043.
Wang, W.X., Wong, R.S.K., 2003. Bioaccumulation kinetics and exposure pathways of inorganic mercury and methylmercury in a marine fish, the sweetlips Plectorhinchus gibbosus. Mar. Ecol. Prog. Ser. 261, 257–268.
Wang, X., Wu, F., Wang, W.X., 2017. In vivo mercury demethylation in a marine fish (Acanthopagrus schlegeli). Environ. Sci. Technol. 51, 6441–6451. https://doi.org/10.1021/acs.est.7b00923.
Wiederhold, J.G., Skyllberg, U., Drott, A., Jiskra, M., Jonsson, S., Björn, E., Bourdon, B., Kretzschmar, R., 2015. Mercury isotope signatures in contaminated sediments as a tracer for local industrial pollution sources. Environ. Sci. Technol. 49, 177–185. https://doi.org/10.1021/es5044358.
Yin, R., Feng, X., Hurley, J.P., Krabbenhoft, D.P., Lepak, R.F., Kang, S., Yang, H., Li, X., 2016. Historical records of mercury stable isotopes in sediments of Tibetan lakes. Sci. Rep. 6, 23332. https://doi.org/10.1038/srep23332.
Zhang, T., Hsu-kim, H., 2010. Photolytic degradation of methylmercury enhanced by binding to natural organic ligands. Nat. Geosci. 3, 473–476. https://doi.org/10.1038/ngeo892.Photolytic.
Zheng, W., Hintelmann, H., 2009. Mercury isotope fractionation during photoreduction in natural water is controlled by its Hg/DOC ratio. Geochem. Cosmochim. Acta 73, 6704–6715. https://doi.org/10.1016/j.gca.2009.08.016.
Živković, I., Kotnik, J., Šolić, M., Horvat, M., 2017. The abundance, distribution and speciation of mercury in waters and sediments of the Adriatic sea - a review. Acta Adriat. 58, 165–186. https://doi.org/10.32582/aa.58.1.14.